Drift Chambers
vs.
Time Projection Chambers

Istituto Nazionale di Fisica Nucleare

F. Grancagnolo

INFN – Lecce

11th FCC-ee workshop: Theory and Experiments

CERN, 8-11 January 2019

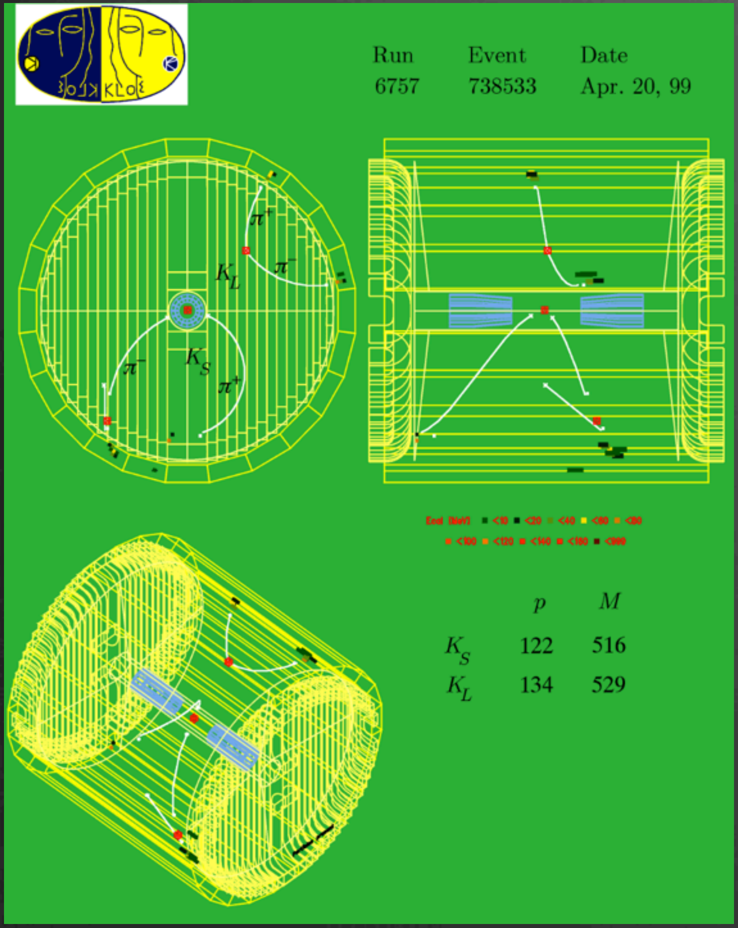
KLOE
Run
6757
Event
738533
Date
Apr. 20, 99
π^+
π^-
K_L
K_S
π^-
π^+
p
M
K_S
122
516
K_L
134
529

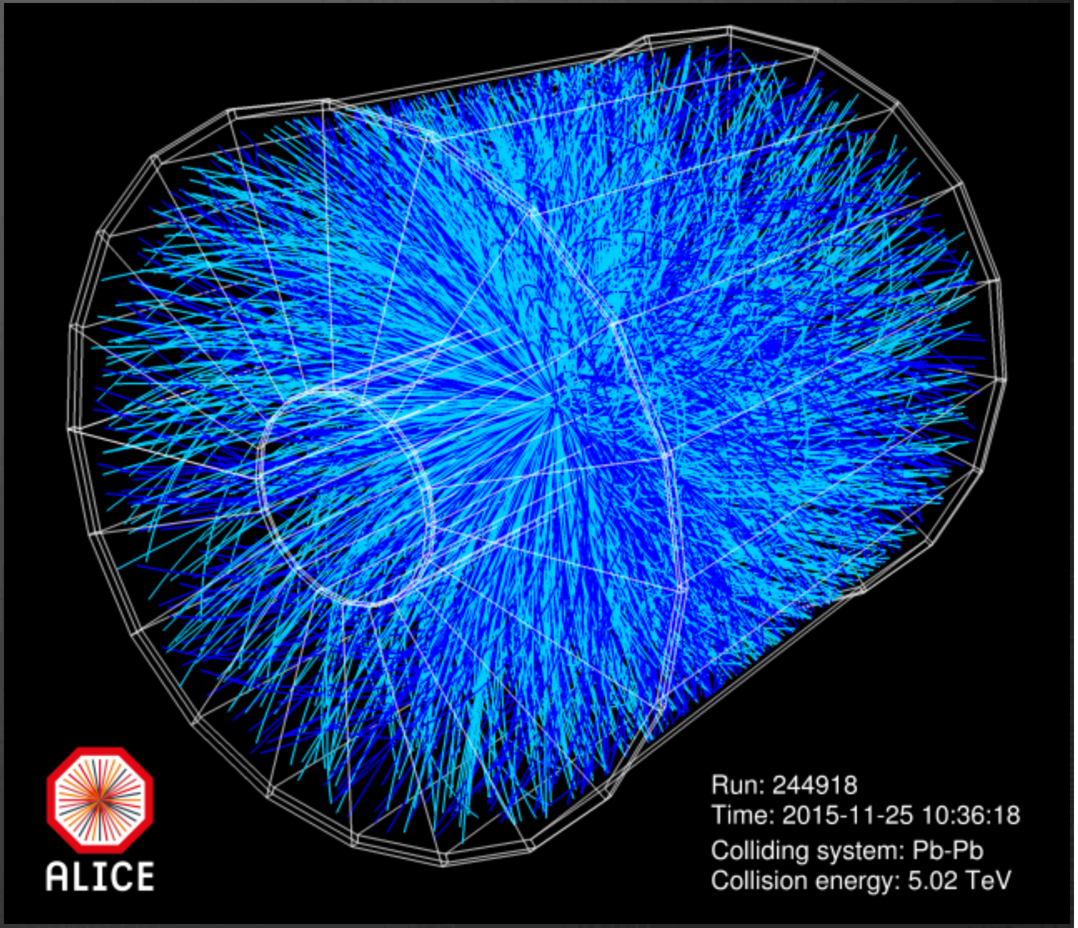
ALICE
Run: 244918
Time: 2015-11-25 10:36:18
Colliding system: Pb-Pb
Collision energy: 5.02 TeV

A due tribute ...

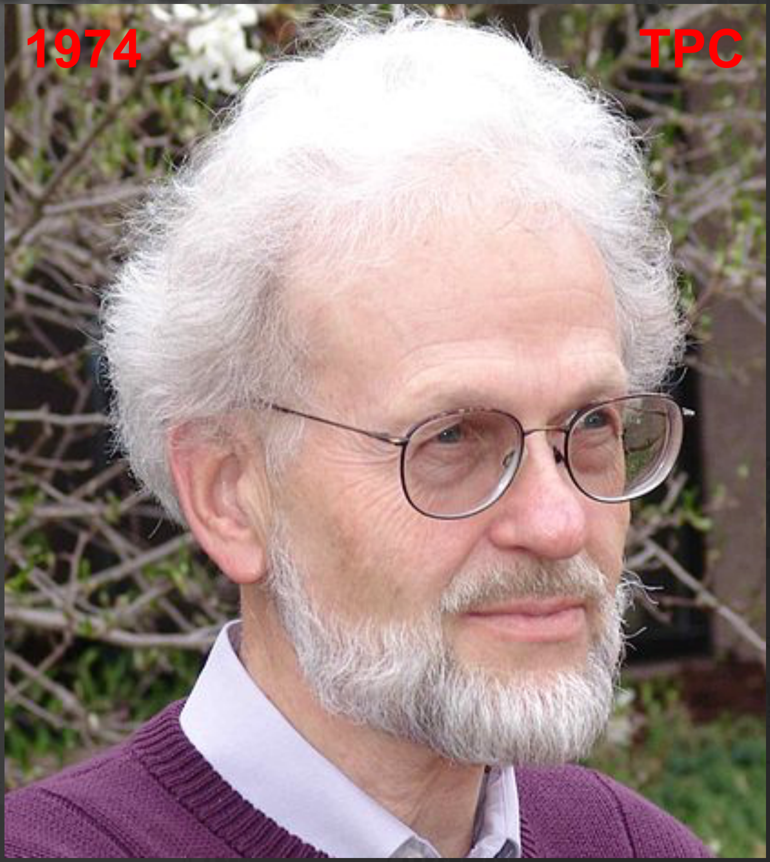

Trackers at e^+e^- colliders

past

SPEAR	MARK2	Drift Chamber
	MARK3	Drift Chamber
DORIS	PLUTO	MWPC
	ARGUS	Drift Chamber
CERS	CLEO1,2	Drift Chamber
PETRA	CELLO	MWPC + Drift Chamber
	JADE	Drift Chamber
	PLUTO	MWPC
	MARK-J	TEC + Drift Chambers
	TASSO	MWPC + Drift Chamber
PEP	MARK2	Drift Chamber
	PEP-4	TPC
	MAC	Drift Chamber
	HRS	Drift Chamber
	DELCO	MWPC + Drift Chamber
TRISTAN	AMY	Drift Chamber
	VENUS	Drift Chamber
	TOPAZ	TPC
BEPC	BES1,2	Drift Chamber

recent past

LEP	ALEPH	TPC
	DELPHI	TPC
	L3	Si + TEC
	OPAL	Drift Chamber
SLC	MARK2	Drift Chamber
	SLD	Drift Chamber
DAPHNE	KLOE	Drift Chamber
VEPP2000	CMD-2	Drift Chamber
PEP2	BaBar	Drift Chamber
KEKB	Belle	Drift Chamber
CESR	CLEO3	Drift Chamber
BEPC2	BES3	Drift Chamber

future

ILC	ILD	TPC
	SiD	Si
CLIC	CLIC	Si
FCC-ee	CLD	Si
	IDEA	Drift Chamber
CEPC	Baseline	TPC Si
	IDEA	Drift Chamber
KEKB	Belle2	Drift Chamber
SCTF	BINP	Drift Chamber
STCF	Hefei	Drift Chamber

Guidelines for tracker choice

- **Fulfillment of physics requirements**
  - Solid angle coverage
  - Detection efficiency (double track separation, vees and kinks, rate capability, aging, front-end electronics response)
  - Ultimate resolutions on angles, momentum, extrapolation to the vertex (including multiple scattering contributions) and particle identification
- **System complexity**
  - Total number of active channels
  - Stability of relative and global alignment
  - Stability of channel to channel calibrations
- **System Interaction**
  - Machine Detector Interface
  - Vertex detector (track extrapolation) and outer electromagnetic calorimeter (tracker transparency)
- **Cost**

Tracker alternatives

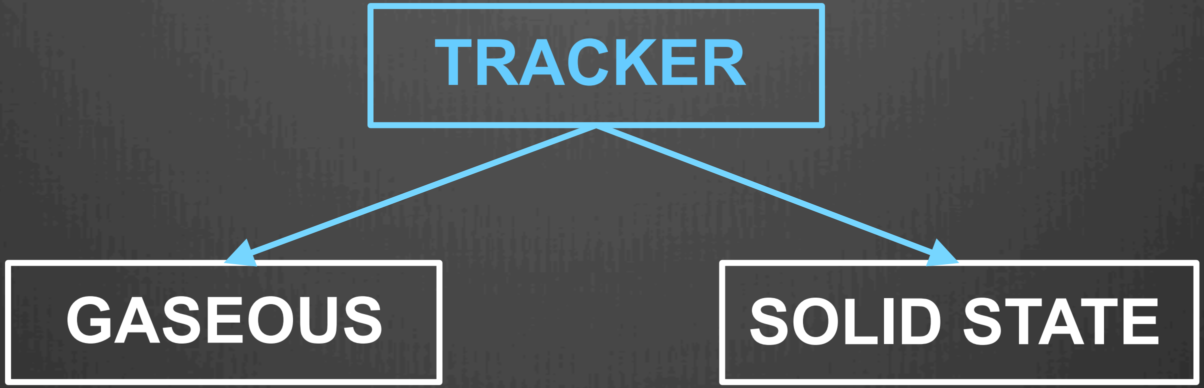

TRACKER

GASEOUS

SOLID STATE

Solid state tracker drawbacks

- **Multiple scattering**

  Contribution to momentum resolution due to multiple scattering dominates up to larger momenta than in a gaseous tracker

- **Redundancy**

  Only a limited number N of layers can be implemented, hindering the momentum resolution, proportional to $\sigma/\sqrt{N}$, despite the excellent spatial resolution σ (is it really needed?) (**$25\ \mu m/\sqrt{6} = 100\ \mu m/\sqrt{100}$**)

  Inefficiencies for "kinks" and "vees"

  Lack of redundancy against hit inefficiencies and background hits

- **particle identification**

  No dE/dx possible, maybe TOF if order of 10 ps resolution can be granted over many m^2

- **system complexity**

  Order of $10^8 – 10^9$ channels for a limited number of space points on a track with a lever arm compatible with the momenta to be measured

  Stability of relative and absolute alignment

Tracker alternatives

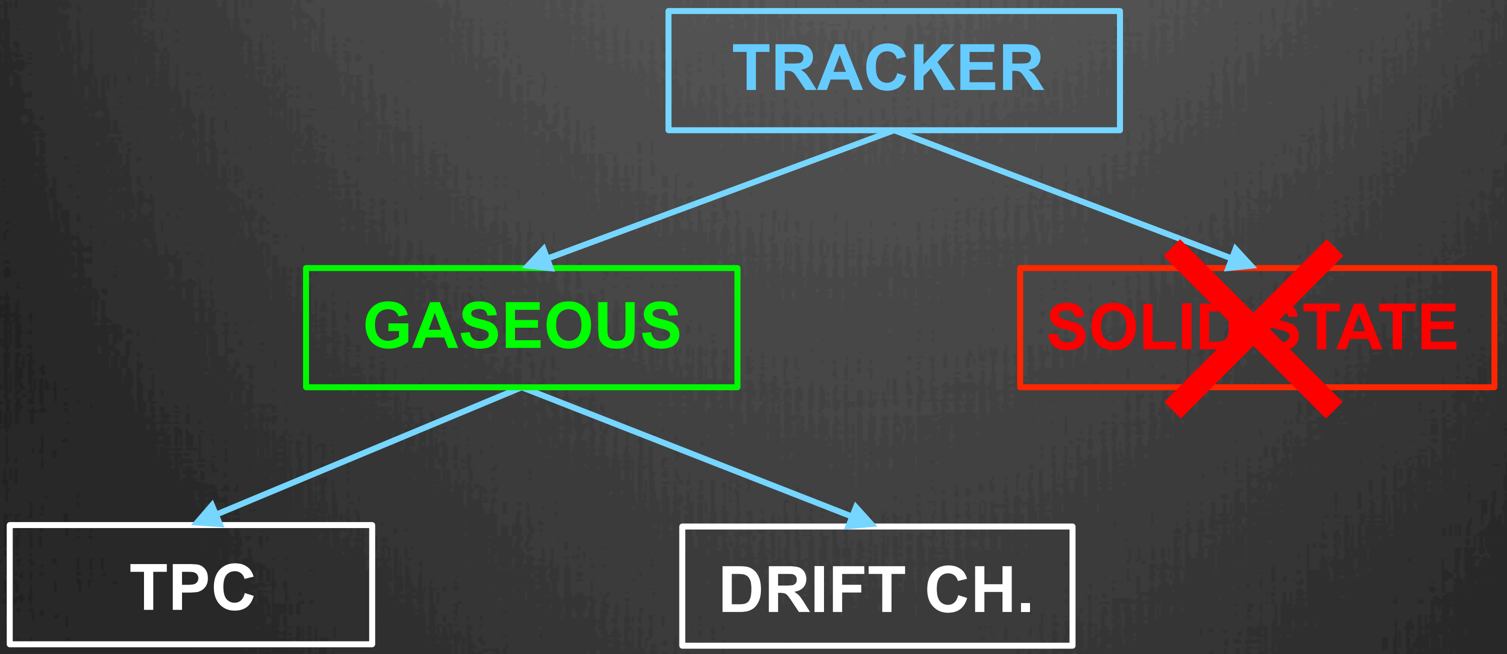

TRACKER

GASEOUS

~~SOLID STATE~~

TPC

DRIFT CH.

TPC of the past at colliders

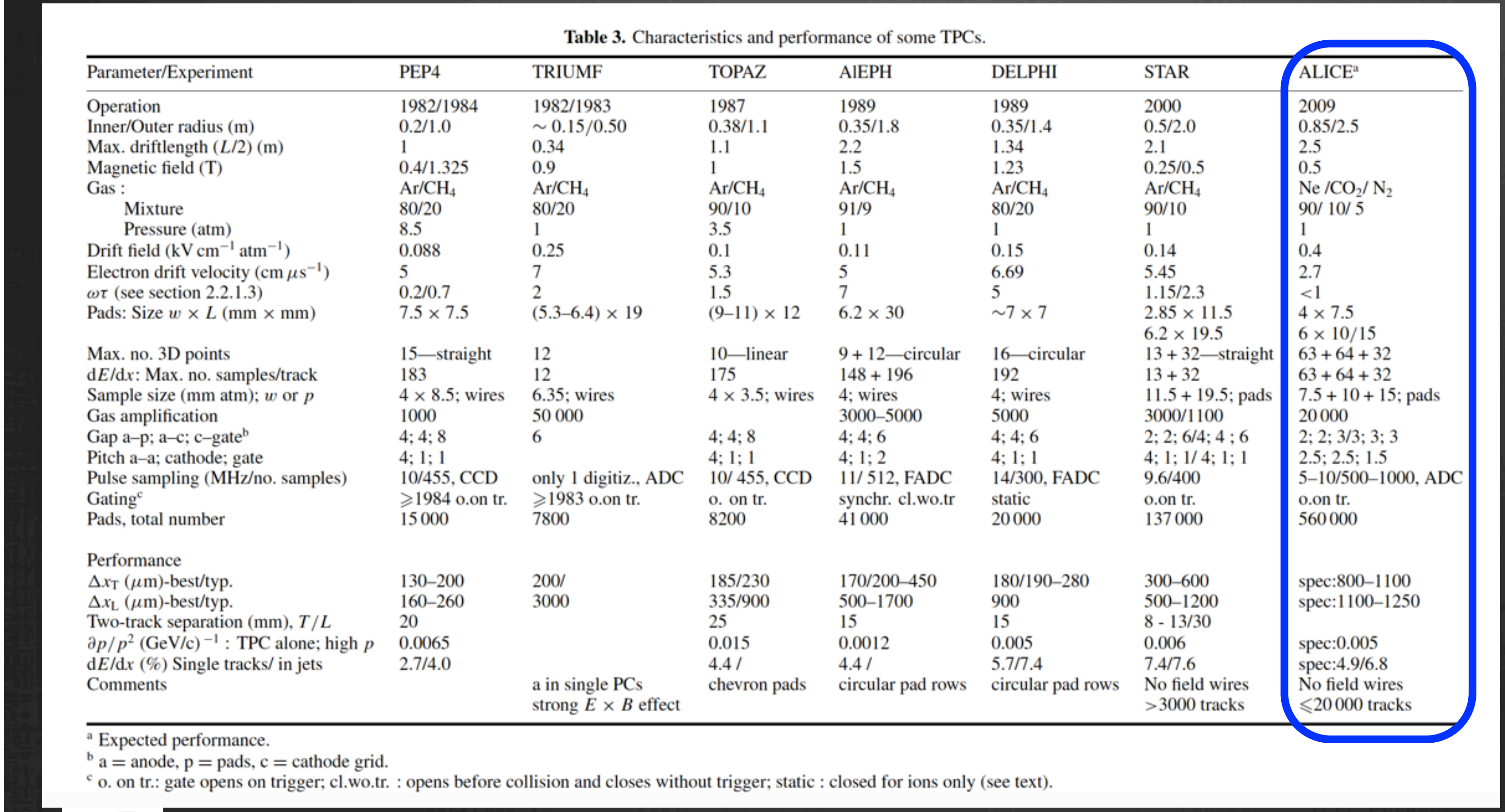

Table 3. Characteristics and performance of some TPCs.

Parameter/Experiment	PEP4	TRIUMF	TOPAZ	AlEPH	DELPHI	STAR	ALICE[a]
Operation	1982/1984	1982/1983	1987	1989	1989	2000	2009
Inner/Outer radius (m)	0.2/1.0	~ 0.15/0.50	0.38/1.1	0.35/1.8	0.35/1.4	0.5/2.0	0.85/2.5
Max. driftlength (*L*/2) (m)	1	0.34	1.1	2.2	1.34	2.1	2.5
Magnetic field (T)	0.4/1.325	0.9	1	1.5	1.23	0.25/0.5	0.5
Gas :	Ar/CH_4	Ar/CH_4	Ar/CH_4	Ar/CH_4	Ar/CH_4	Ar/CH_4	$Ne/CO_2/N_2$
Mixture	80/20	80/20	90/10	91/9	80/20	90/10	90/ 10/ 5
Pressure (atm)	8.5	1	3.5	1	1	1	1
Drift field ($kV\,cm^{-1}\,atm^{-1}$)	0.088	0.25	0.1	0.11	0.15	0.14	0.4
Electron drift velocity ($cm\,\mu s^{-1}$)	5	7	5.3	5	6.69	5.45	2.7
$\omega\tau$ (see section 2.2.1.3)	0.2/0.7	2	1.5	7	5	1.15/2.3	<1
Pads: Size $w \times L$ (mm × mm)	7.5 × 7.5	(5.3–6.4) × 19	(9–11) × 12	6.2 × 30	~7 × 7	2.85 × 11.5 6.2 × 19.5	4 × 7.5 6 × 10/15
Max. no. 3D points	15—straight	12	10—linear	9 + 12—circular	16—circular	13 + 32—straight	63 + 64 + 32
dE/dx: Max. no. samples/track	183	12	175	148 + 196	192	13 + 32	63 + 64 + 32
Sample size (mm atm); w or p	4 × 8.5; wires	6.35; wires	4 × 3.5; wires	4; wires	4; wires	11.5 + 19.5; pads	7.5 + 10 + 15; pads
Gas amplification	1000	50 000		3000–5000	5000	3000/1100	20 000
Gap a–p; a–c; c–gate[b]	4; 4; 8	6	4; 4; 8	4; 4; 6	4; 4; 6	2; 2; 6/4; 4 ; 6	2; 2; 3/3; 3; 3
Pitch a–a; cathode; gate	4; 1; 1		4; 1; 1	4; 1; 2	4; 1; 1	4; 1; 1/ 4; 1; 1	2.5; 2.5; 1.5
Pulse sampling (MHz/no. samples)	10/455, CCD	only 1 digitiz., ADC	10/ 455, CCD	11/ 512, FADC	14/300, FADC	9.6/400	5–10/500–1000, ADC
Gating[c]	⩾1984 o.on tr.	⩾1983 o.on tr.	o. on tr.	synchr. cl.wo.tr	static	o.on tr.	o.on tr.
Pads, total number	15 000	7800	8200	41 000	20 000	137 000	560 000
Performance							
Δx_T (μm)-best/typ.	130–200	200/	185/230	170/200–450	180/190–280	300–600	spec:800–1100
Δx_L (μm)-best/typ.	160–260	3000	335/900	500–1700	900	500–1200	spec:1100–1250
Two-track separation (mm), T/L	20		25	15	15	8 - 13/30	
$\partial p/p^2$ $(GeV/c)^{-1}$: TPC alone; high p	0.0065		0.015	0.0012	0.005	0.006	spec:0.005
dE/dx (%) Single tracks/ in jets	2.7/4.0		4.4 /	4.4 /	5.7/7.4	7.4/7.6	spec:4.9/6.8
Comments		a in single PCs strong $E \times B$ effect	chevron pads	circular pad rows	circular pad rows	No field wires >3000 tracks	No field wires ⩽20 000 tracks

[a] Expected performance.

[b] a = anode, p = pads, c = cathode grid.

[c] o. on tr.: gate opens on trigger; cl.wo.tr. : opens before collision and closes without trigger; static : closed for ions only (see text).

from

H. J. Hilke

Rep. Prog. Phys. 72 (2010) 116201

ALICE TPC performance

In Pb-Pb collisions (dN/dη = 8000, N = 20,000)   40% (15%) **occupancy** at innermost (outermost) radius

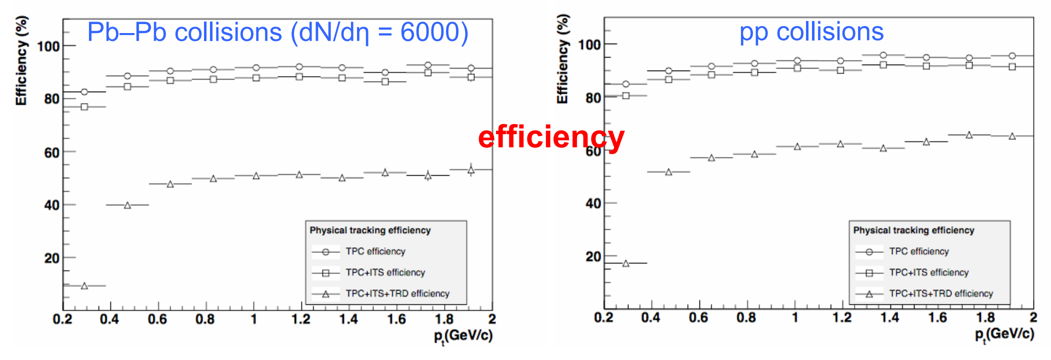

efficiency

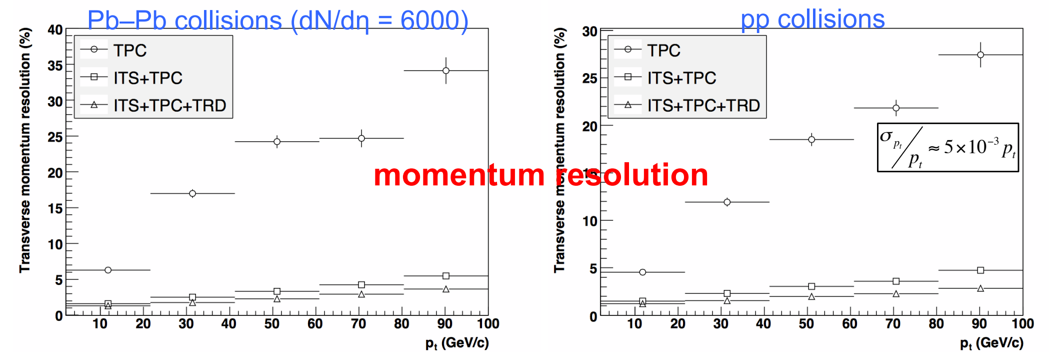

$$\sigma_{p_t}/p_t \approx 5\times10^{-3}\,p_t$$

momentum resolution

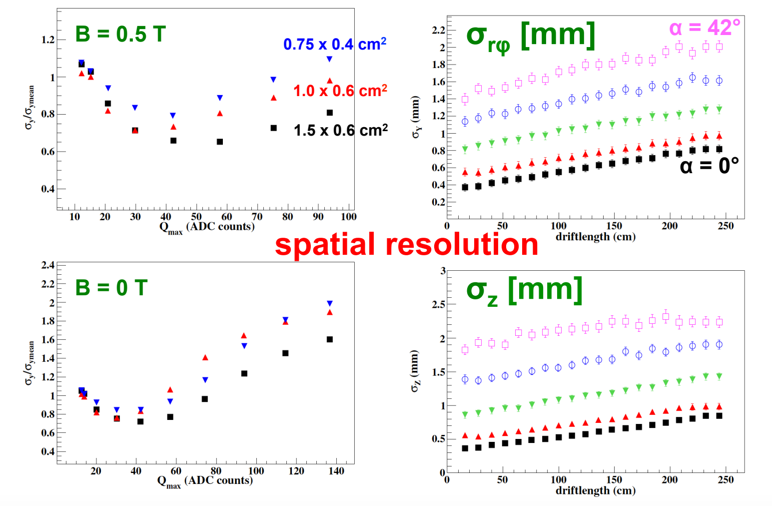

spatial resolution

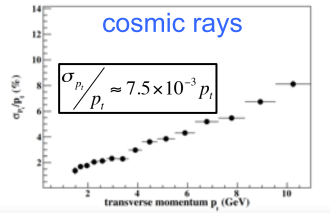

$$\sigma_{p_t}/p_t \approx 7.5\times10^{-3}\,p_t$$

ALICE TPC performance

kink finding efficiency

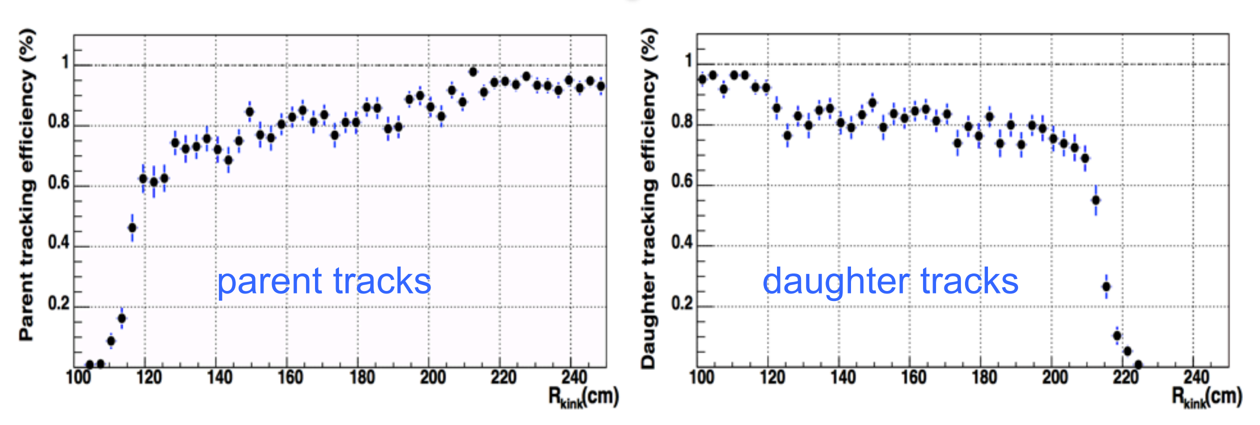

particle identification

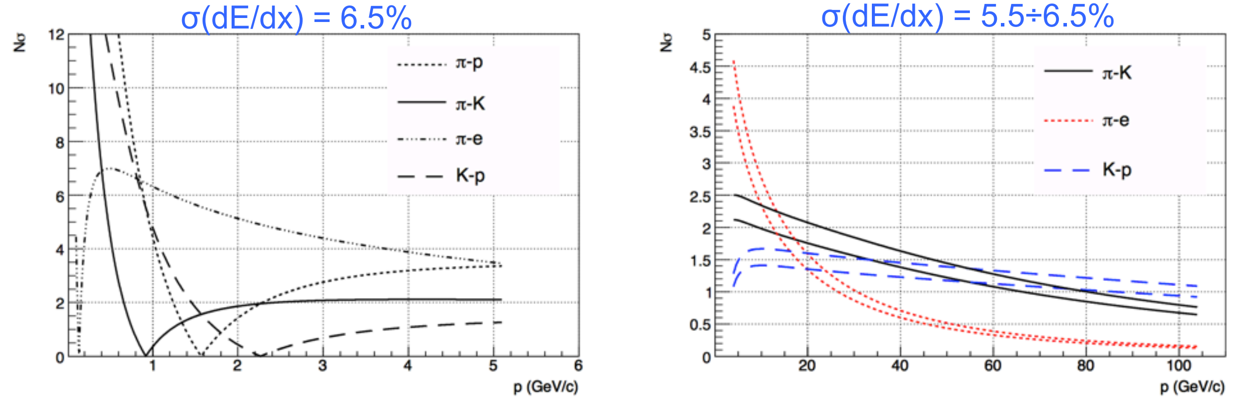
σ(dE/dx) = 6.5%

σ(dE/dx) = 5.5÷6.5%

Cost of performance: **complexity**

Field Cage

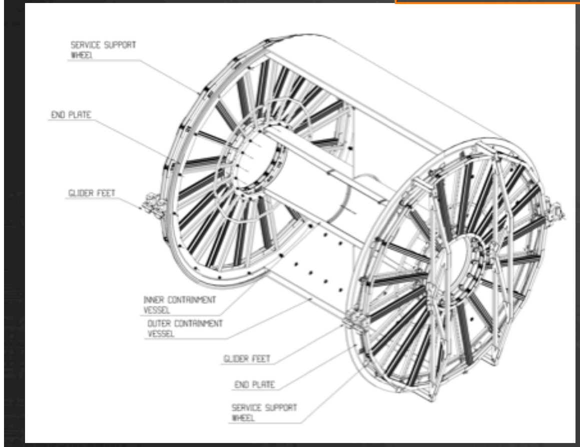

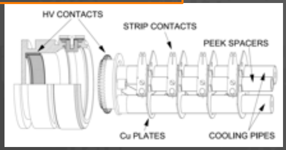

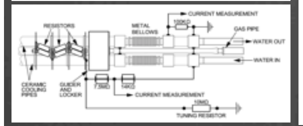

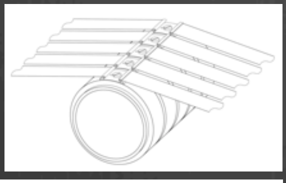

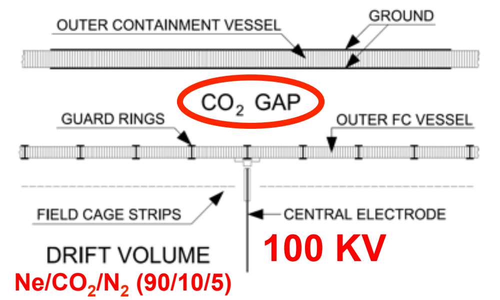

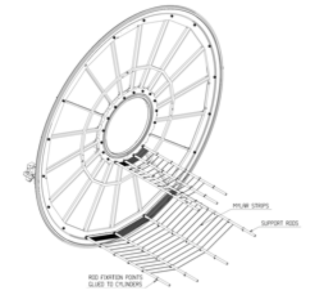

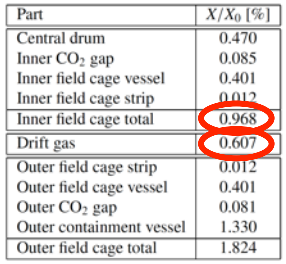

Part	X/X_0 [%]
Central drum	0.470
Inner CO_2 gap	0.085
Inner field cage vessel	0.401
Inner field cage strip	0.012
Inner field cage total	0.968
Drift gas	0.607
Outer field cage strip	0.012
Outer field cage vessel	0.401
Outer CO_2 gap	0.081
Outer containment vessel	1.330
Outer field cage total	1.824

total 3.4%

Field Cage	6.0 ton
ROC + cool.	2.6 ton
SSW	5.6 ton
Total	**14.2 ton**

2 × 166 Strips

72 Rods

- resistor rods (water cooled)
- HV cable rods
- laser rods
- gas rods

MWPC

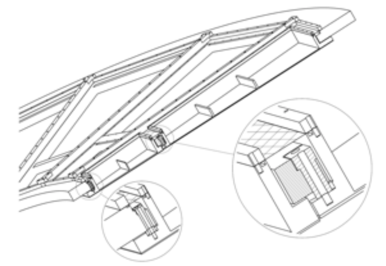

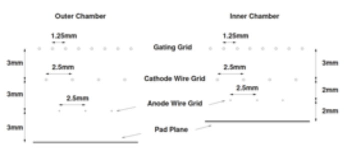

72 MWPC
100,000 wires
560,000 RO pads

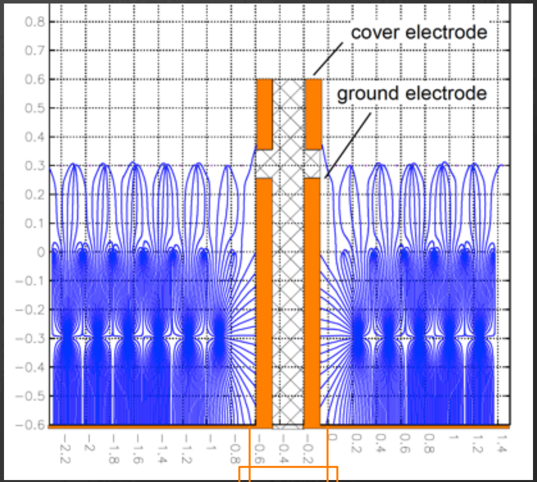

dead area (10%)

Gate closed.
Opens on trigger
for 90 μs

IFB Gating efficiency
< 0.7 × 10^{-4}
(g = 2 × 10^4)

Cost of performance: **complexity**

Implications of a long drift distance (2.5 m)

- **Drift field** (400 V/cm) distortions at **10^{-4}** level contribute with **250 µm** to spatial resolution
- **Temperature** stability **< 0.1°K**, corresponding to **≈1mm** for vdrift = 2.65 cm/µs, necessitates a **complex cooling systems** (HV distribution and FEE)
- **$\Delta v_{drift}/v_{drift} = -6.4\times\Delta(CO_2)/(CO_2) = -1.0\times\Delta(N_2)/(N_2) < 10^{-4}$** implies $\Delta(CO_2)/(CO_2) < 0.01\%$! **gas chromatograph + thermal conductivity detector + high precision drift velocity monitoring** necessary
- **5 ppm of O_2** attach **25% of electrons** after 2.5 m drift. Gas tightness and fresh gas flow rate (high cost of Ne) are critical

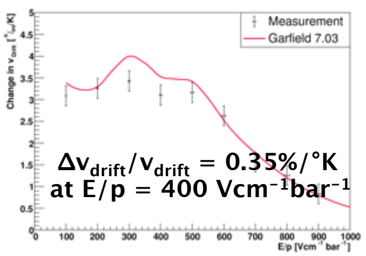

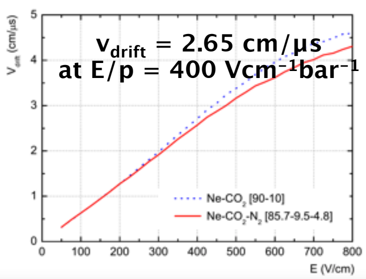

Calibrations: lasers and radioactive sources

- **Two 150 mJ/5 ns pulse Nd:YAG lasers (266 nm)** are split in **336 synchronous beams** by means of remotely controlled systems of mirrors, beam splitters and bending prisms (Δx, Δy, Δz ≤ 800−1000 µm; Δϑ, Δφ ≤ 0.4−0.5 mrad), monitored by a calibrated energy meter and imaged with a CCD. Moreover, laser beams reflected by metallic surfaces (HV strips) define maximum drift time.
- **Radioactive Kr gas** is used for **pad-by-pad calibration by equalizing gain at 1.5%**

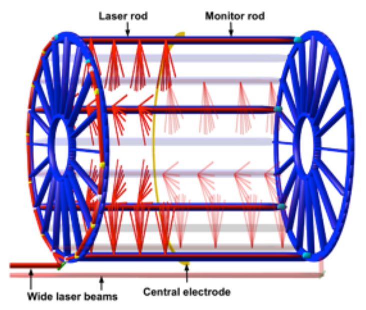

... from ALICE to CEPC-TPC

Un-gated TPC with MPGD readout

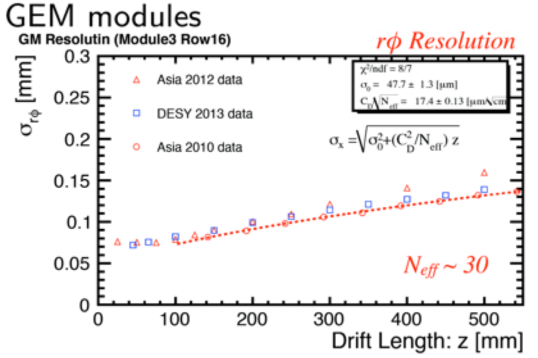

from LC-TPC Collaboration

extrapolated to CEPC-TPC (2.2 m drift)

gives 250 μm and 120 equivalent 3D points

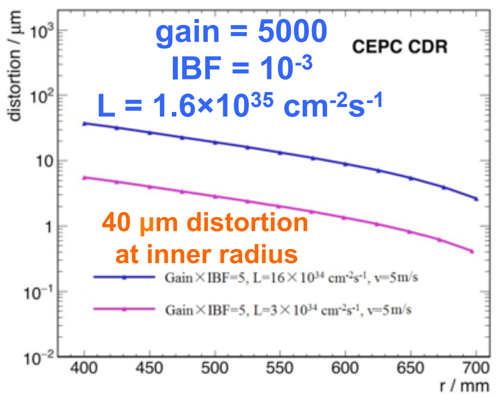

gain = 5000

IBF = 10^{-3}

L = 1.6×10^{35} $cm^{-2}s^{-1}$

CEPC CDR

40 μm distortion
at inner radius

A combination of GEM and MM

- pad granularity: 1 mm × 6mm
  ≈ 2 million channels R.O.
- gas gain: 5×10^3
- IFB suppression: 10^{-3} (intrinsic)
- gas: T2K ($Ar/CF_4/iC_4H_{10}$ = 92/7/1)
- power consumption: < 5 mW/ch

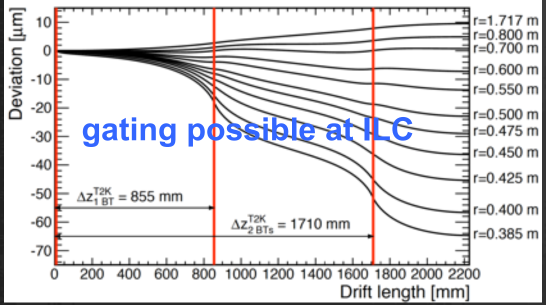

gating possible at ILC

from LC-TPC Collaboration

ILC beam time structure

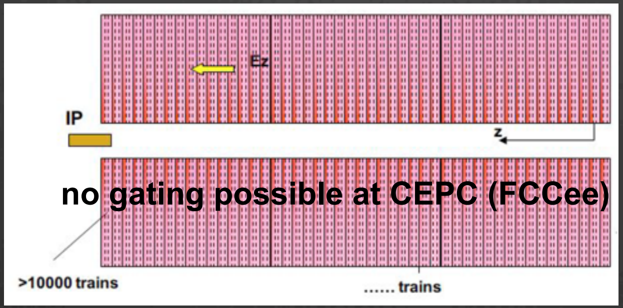

no gating possible at CEPC (FCCee)

from CEPC CDR

≈ continuous CEPC (FCCee) beam time structure

All other issue regarding the complexity of running such a critically delicate detector remain open

... from ALICE to CEPC-TPC

Field Cage: complexity of operability
mechanical structure (> 14 ton)
cooling issues

Laser alignment

Pad by pad calibration stability (aggravated by the larger number of pads)

Gas issues: drift field distortions must be kept within a factor 4 below 10^{-4}
because of a factor four better (claimed) spatial resolution
temperature stability much better than 0.1°K
drift velocity monitoring to better than 10^{-4}
oxygen content below 5 ppm concentration

Low discharge and sparking possibilities typical of MPGD

B-field: what if B = 3T turns out to be incompatible and needs to be reduced to 2T?
What happens to spatial resolution?

Drift Chambers of the past at colliders

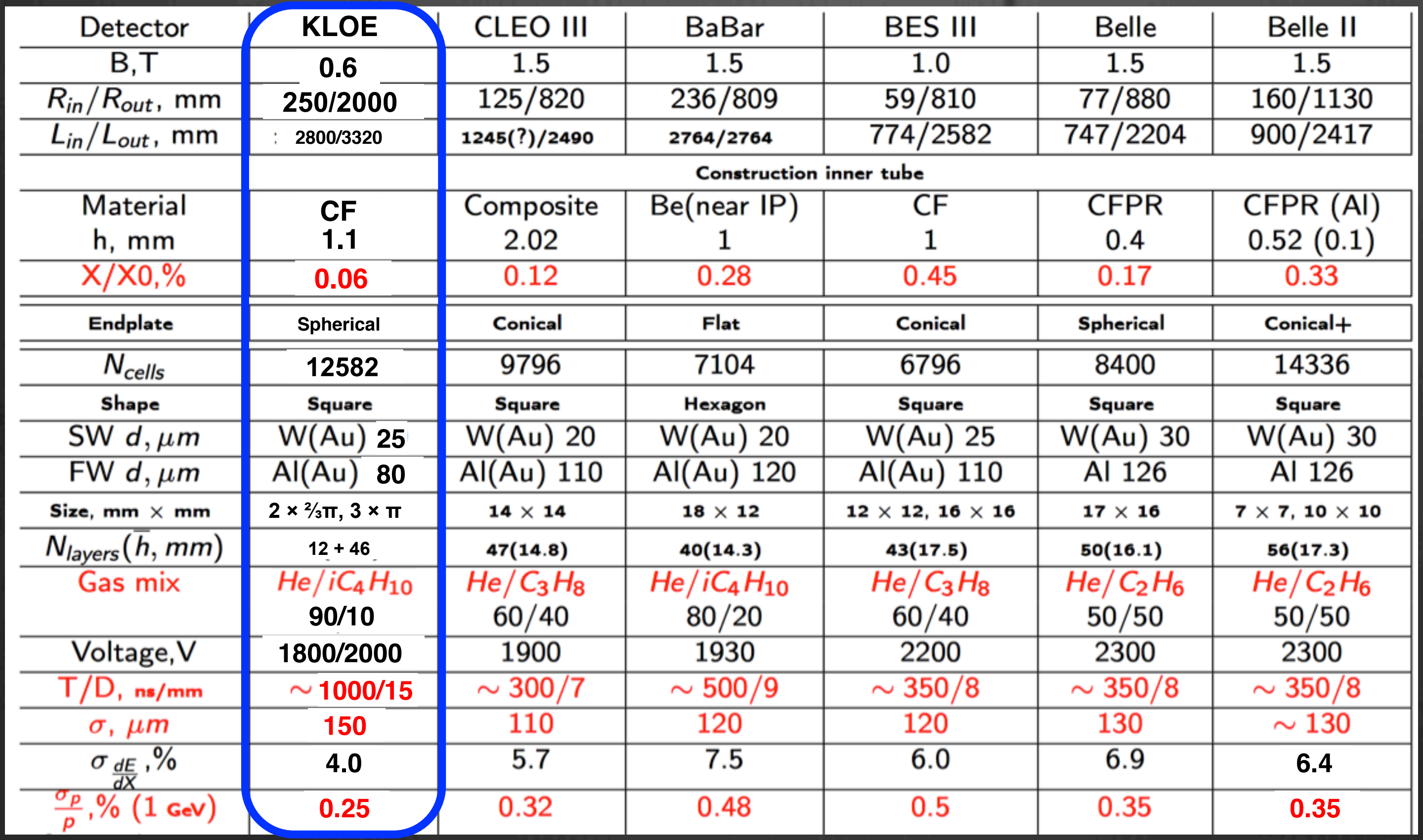

Detector	KLOE	CLEO III	BaBar	BES III	Belle	Belle II
B,T	0.6	1.5	1.5	1.0	1.5	1.5
R_{in}/R_{out}, mm	250/2000	125/820	236/809	59/810	77/880	160/1130
L_{in}/L_{out}, mm	2800/3320	1245(?)/2490	2764/2764	774/2582	747/2204	900/2417
		Construction inner tube				
Material h, mm	CF 1.1	Composite 2.02	Be(near IP) 1	CF 1	CFPR 0.4	CFPR (Al) 0.52 (0.1)
X/X0,%	0.06	0.12	0.28	0.45	0.17	0.33
Endplate	Spherical	Conical	Flat	Conical	Spherical	Conical+
N_{cells}	12582	9796	7104	6796	8400	14336
Shape	Square	Square	Hexagon	Square	Square	Square
SW $d, \mu m$	W(Au) 25	W(Au) 20	W(Au) 20	W(Au) 25	W(Au) 30	W(Au) 30
FW $d, \mu m$	Al(Au) 80	Al(Au) 110	Al(Au) 120	Al(Au) 110	Al 126	Al 126
Size, mm × mm	2 × ⅔π, 3 × π	14 × 14	18 × 12	12 × 12, 16 × 16	17 × 16	7 × 7, 10 × 10
$N_{layers}(\bar{h}, mm)$	12 + 46	47(14.8)	40(14.3)	43(17.5)	50(16.1)	56(17.3)
Gas mix	He/iC_4H_{10} 90/10	He/C_3H_8 60/40	He/iC_4H_{10} 80/20	He/C_3H_8 60/40	He/C_2H_6 50/50	He/C_2H_6 50/50
Voltage,V	1800/2000	1900	1930	2200	2300	2300
T/D, ns/mm	~1000/15	~ 300/7	~ 500/9	~ 350/8	~ 350/8	~ 350/8
σ, μm	150	110	120	120	130	~ 130
$\sigma_{\frac{dE}{dX}}$,%	4.0	5.7	7.5	6.0	6.9	6.4
$\frac{\sigma_p}{p}$,% (1 GeV)	0.25	0.32	0.48	0.5	0.35	0.35

from

Todishev - Basok

Future tau-charm, Orsay Dec. 2018

KLOE Drift Chamber performance

spatial resolution

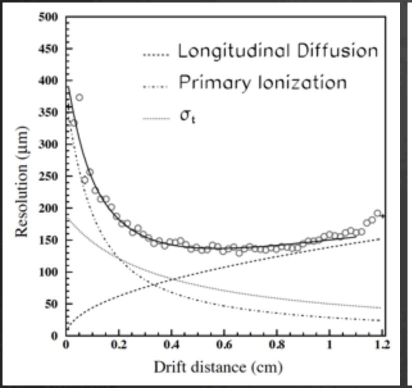

hit efficiency

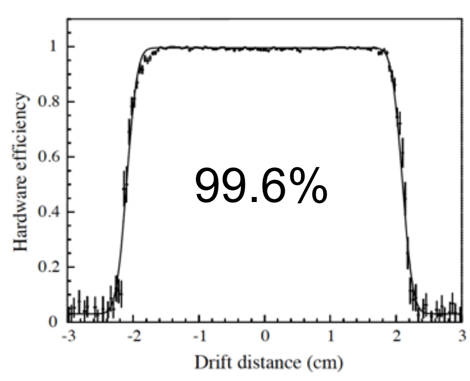

hit-track assignment

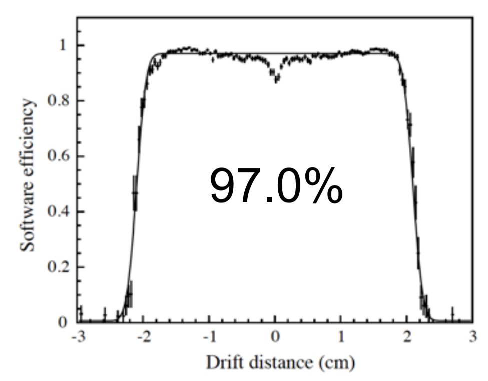

momentum resolution

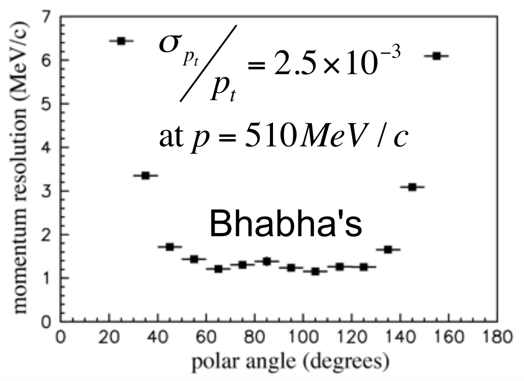

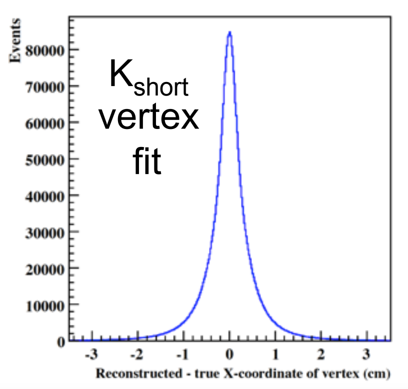

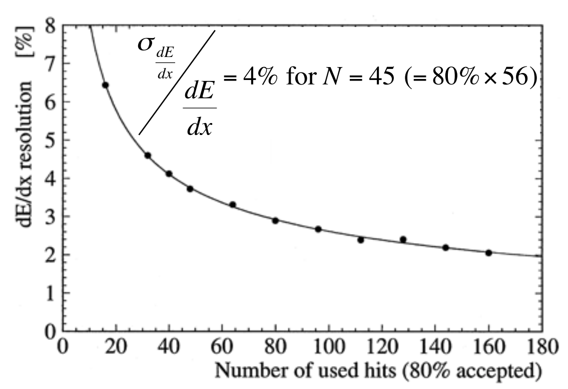

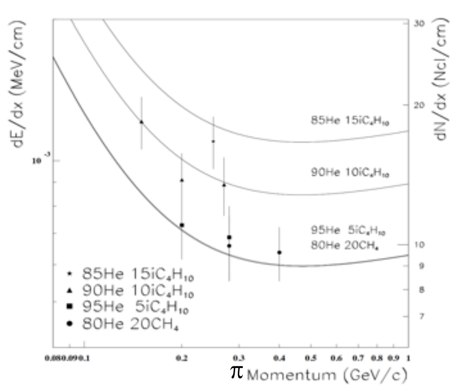

Cost of performance: **t-to-d relation**

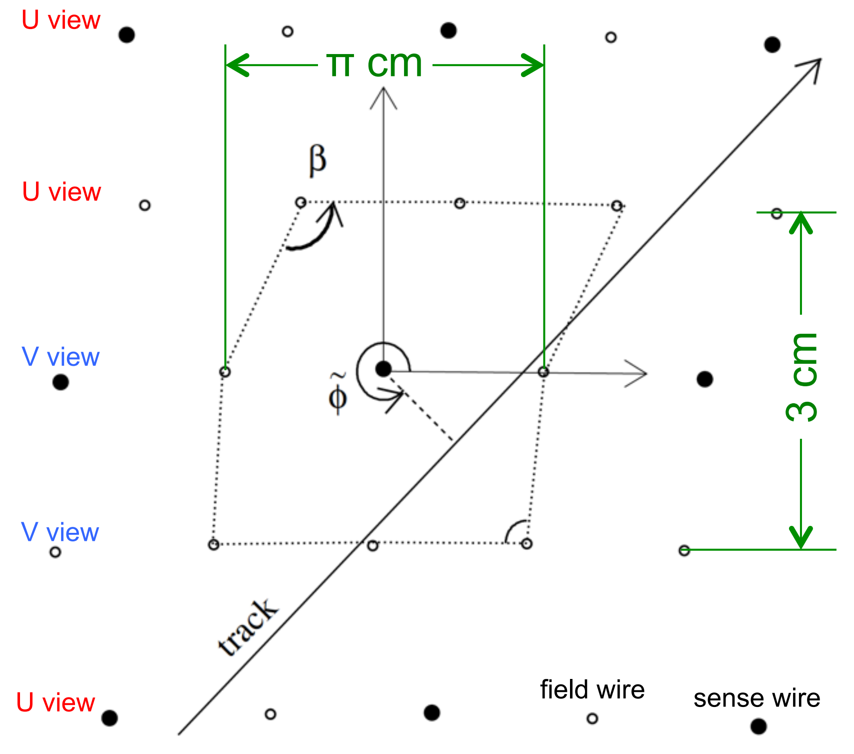

"almost" square cell require **t-to-d angle dependent**

Layer at outer bound of cell aims at opposite sign stereo angle w.r.t. sense wire layer and layer at inner bound implying **t-to-d relations are functions of the track angle and the cell periodicity in z**.

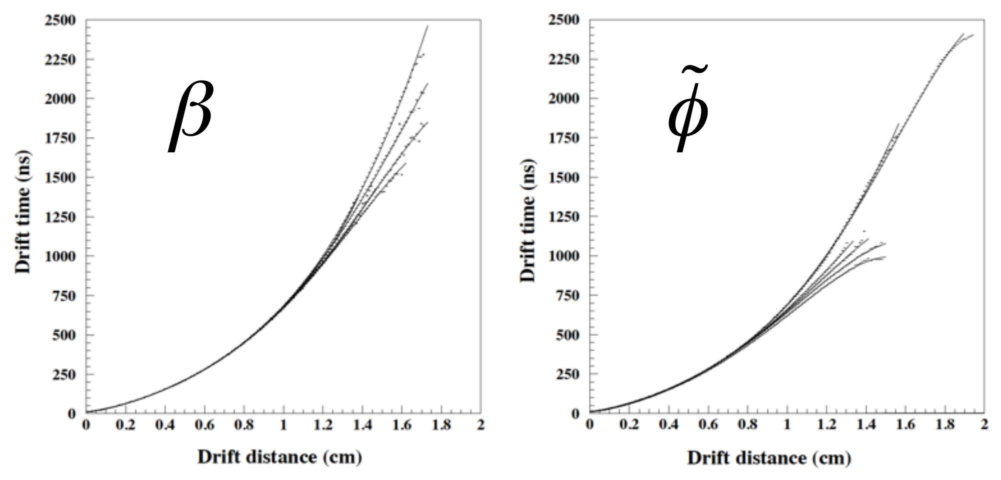

Cost of performance: **stereo angle**

Three possible configurations:

- constant **stereo angle ε** for all layers
- constant **angular displacement α**
- constant **stereo drop δ**

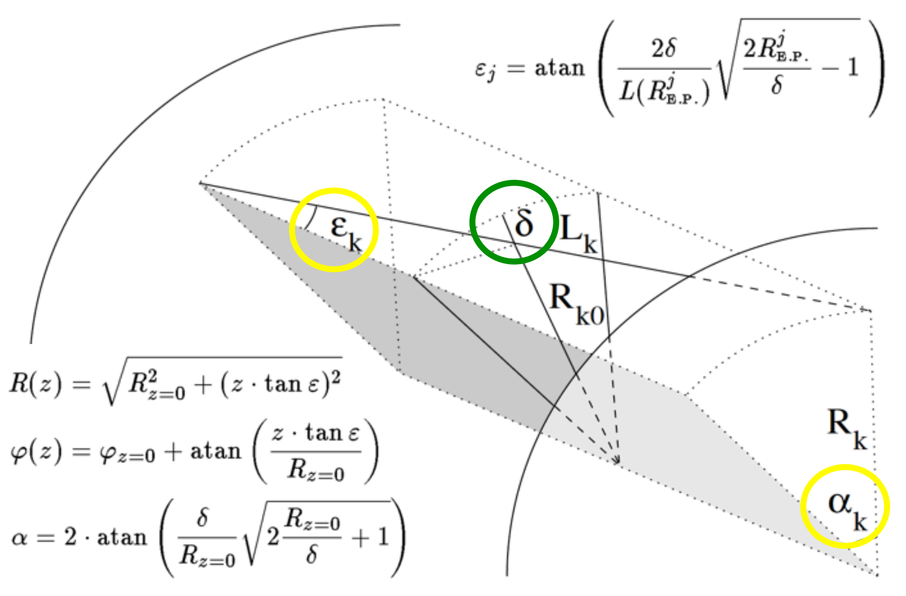

$$\varepsilon_j = \mathrm{atan}\left(\frac{2\delta}{L(R^j_{\mathrm{E.P.}})}\sqrt{\frac{2R^j_{\mathrm{E.P.}}}{\delta} - 1}\right)$$

$$R(z) = \sqrt{R^2_{z=0} + (z \cdot \tan\varepsilon)^2}$$

$$\varphi(z) = \varphi_{z=0} + \mathrm{atan}\left(\frac{z \cdot \tan\varepsilon}{R_{z=0}}\right)$$

$$\alpha = 2 \cdot \mathrm{atan}\left(\frac{\delta}{R_{z=0}}\sqrt{2\frac{R_{z=0}}{\delta} + 1}\right)$$

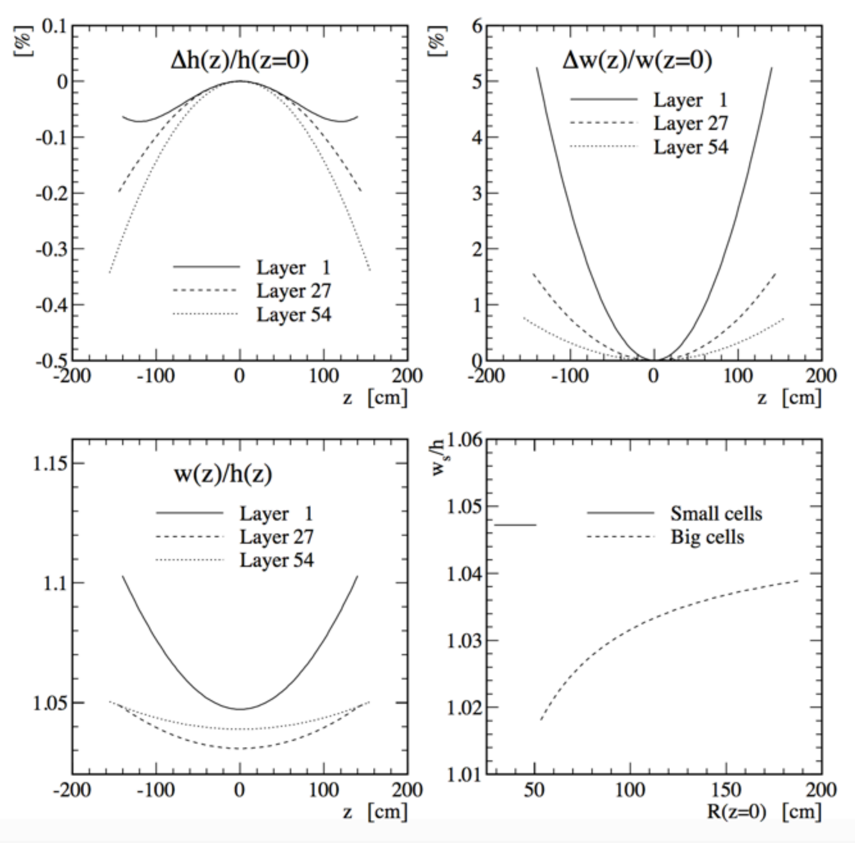

... from KLOE to IDEA

Stereo configuration with **constant angular displacement α**

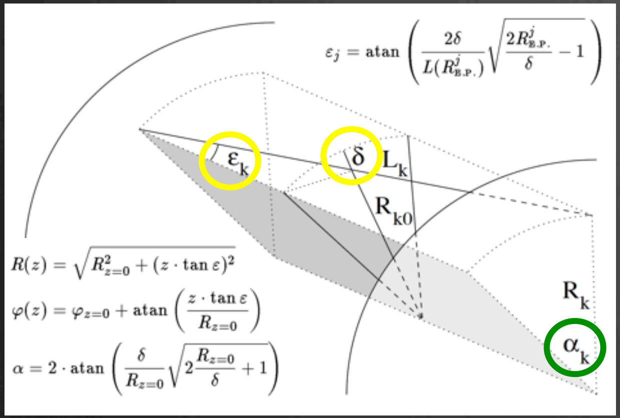

$$\varepsilon_j = \text{atan}\left(\frac{2\delta}{L(R^j_{\text{E.P.}})}\sqrt{\frac{2R^j_{\text{E.P.}}}{\delta} - 1}\right)$$

$$R(z) = \sqrt{R^2_{z=0} + (z \cdot \tan\varepsilon)^2}$$

$$\varphi(z) = \varphi_{z=0} + \text{atan}\left(\frac{z \cdot \tan\varepsilon}{R_{z=0}}\right)$$

$$\alpha = 2 \cdot \text{atan}\left(\frac{\delta}{R_{z=0}}\sqrt{2\frac{R_{z=0}}{\delta} + 1}\right)$$

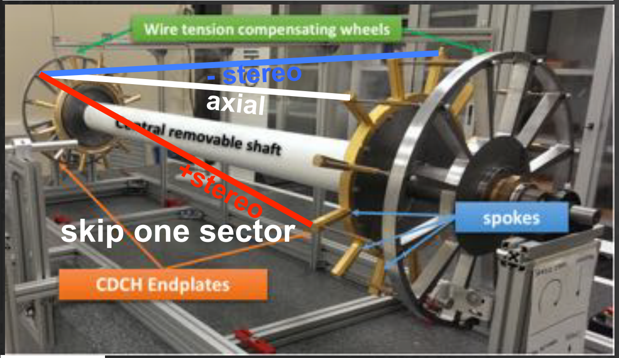

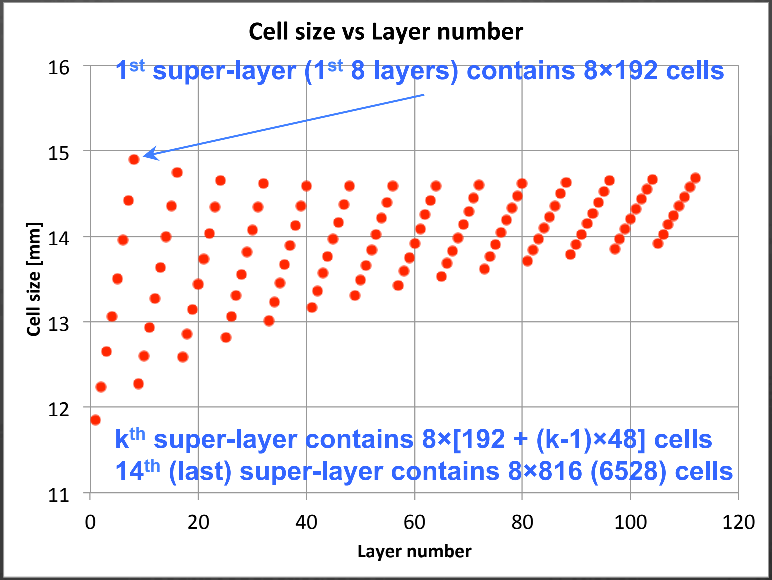
Cell size vs Layer number

1st super-layer (1st 8 layers) contains 8×192 cells

kth super-layer contains 8×[192 + (k-1)×48] cells

14th (last) super-layer contains 8×816 (6528) cells

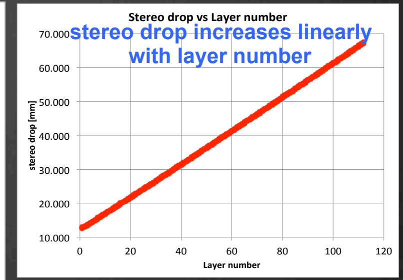
Stereo drop vs Layer number

stereo drop increases linearly with layer number

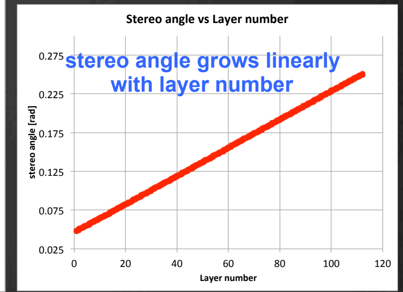
Stereo angle vs Layer number

stereo angle grows linearly with layer number

Issues still remaining open (see a few slides ahead):

- **wire electrostatics stability over 4 m length**
- **inner layers occupancy**
- **data rate transfer for cluster counting/timing**

... from KLOE to IDEA

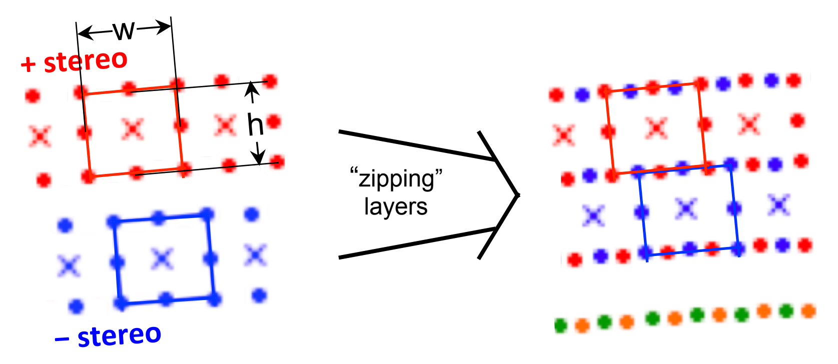

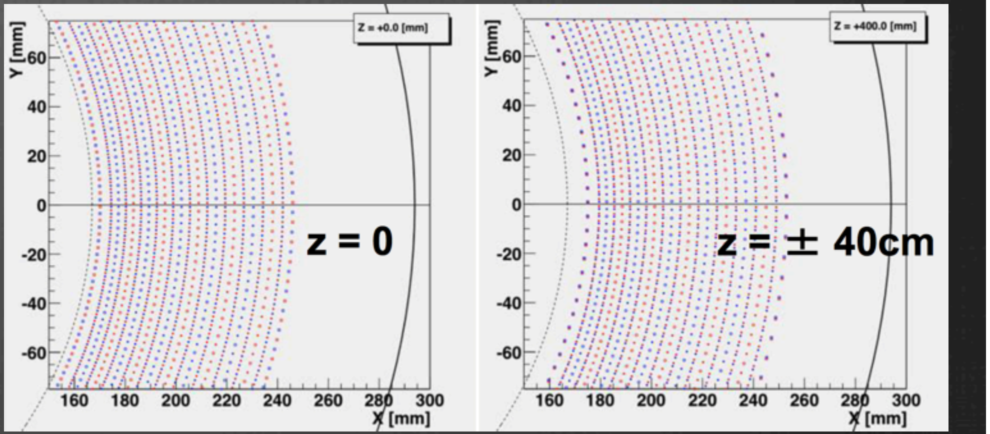

perfectly "square" cells: $w_i = h_i$ at any z:
$w_i(z=L/2) = h_i(z=L/2) = 1.035\ w_i(z=0) = 1.035\ h_i(z=0)$
no β angle dependence
no Φ angle dependence
in principle, one single t-to-d scalable for all layers

Configuration used for MEG2 chamber

Configuration requires more field w. per sense w. (5:1, as opposed to 3:1 in KLOE) allowing for thinner field wires, therefore less m.s. contribution and less mechanical tension on end plates.

Requires automatized feed-through-less wiring procedure, already used for the MEG2 chamber

... from KLOE to IDEA

Limited number of sensitive elements (< 60,000 sense wires) sampled at high rate (2 GSa/s) over the maximum drift time (40 ns) allows for:

- **cluster timing** for improving spatial resolution at small impact parameters
- **cluster counting** for excellent particle identification (no need for fancy pulse height calibration)
- **fast hit filtering** and **efficient compression** of raw data
- **bunch crossing identification** within a few ns

Occupancy issues have been addressed with simulations both at Z and top energies within the FCC-ee framework confirming a relatively safe environment

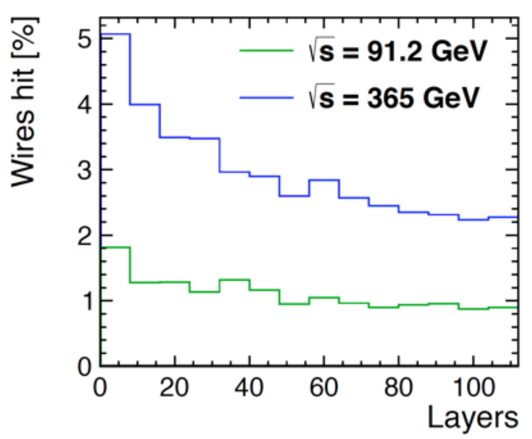

... from KLOE to IDEA

Sense wires electrostatic stability

$$C = \frac{2\pi\varepsilon}{\ln\left(\frac{\{2\}w}{2r}\right)}$$

sense wire
capacitance
per unit length
C = 8 pF/m

$$T > \frac{C^2 V_0^2 L^2}{4\pi\varepsilon w^2}$$

IDEA sense wires stability condition

T > 0.14 N

0.14 N for a 20 μm W sense wire correspond to **450 MPa**, very close to the W yield strength (elastic limit) = **750 MPa**.

Analogously for the Al field wires, one gets **175 MPa**, as opposed to the Al yield strength of **275 MPa**.

Both present a mere **1.5 safety factor** against failure! Is it safe enough? Most chamber have been operated at an even smaller safety factor.

... from KLOE to IDEA

However ...

SPECIALTY MATERIALS, INC.

Manufacturers of Boron and SCS Silicon Carbide Fibers and Boron Nanopowder

CARBON MONOFILAMENT

TYPICAL PROPERTIES

Diameter:	0.00136 +/- 0.0001" (34.5 +/- 2.5 μm)
Tensile Strength:	125 ksi (0.86 GPa)
Tensile Modulus:	6 msi (41.5 GPa)
Electrical Resistivity:	3.6 x 10^{-3} ohm cm
Density:	1.8 g/cc

Specialty Materials, Inc.
1449 Middlesex Street
Lowell, Massachusetts 01851

Phone: 978-322-1900
Fax: 978-322-1970

CARBON MONOFILAMENT PRODUCT PRICE LIST
Effective October 1, 2017

Product	Quantity	Price LF
CARBON MONOFILAMENT	1 Million LF	$0.02
	500,000 LF	$0.03
	1,000 LF	$0.93

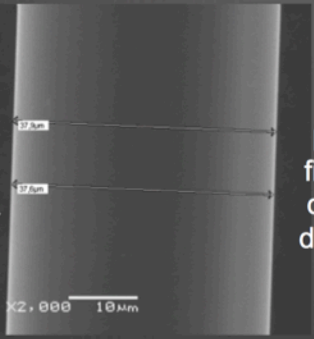

High-power impulse magnetron sputtering (HiPIMS)

physical vapor deposition of thin films based on magnetron sputter deposition (extremely high power densities of the order of kW/cm^2 in short pulses of tens of μs at low duty cycle <10%)

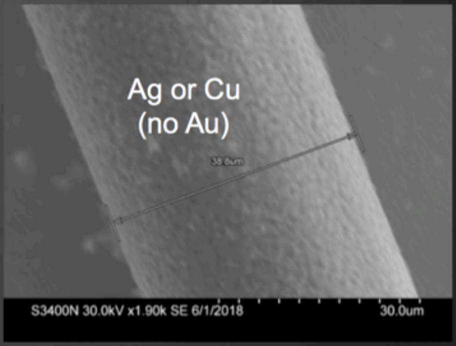

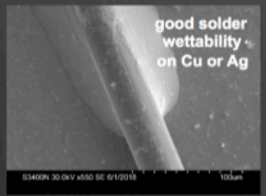

thanks to A. Popov - V. Logashenko, BINP